

## One-step Synthesis of Hierarchically Porous Silicas with Multilamellar Vesicular Core and Ordered Mesostructured Shell

Pei Yuan<sup>1,2</sup> and Chengzhong Yu\*<sup>1,2</sup>

<sup>1</sup>ARC Centre of Excellence for Functional Nanomaterials, The University of Queensland, Brisbane, QLD 4072, Australia

<sup>2</sup>Australian Institute for Bioengineering and Nanotechnology, The University of Queensland, Brisbane, QLD 4072, Australia

(Received March 17, 2011; CL-110232; E-mail: c.yu@uq.edu.au)

Hierarchically porous silicas with multilamellar vesicular core and ordered mesostructured shell have been successfully synthesized using a simple one-step method through a soft dual-templating approach. The vesicular core has irregular cavity size generally larger than 100 nm, while the pore size of the shell is 9.8 nm, which may have potential applications in loading and controlled release of large molecules.

Recently, designed fabrication of hierarchically porous silicas (HPSs) have attracted increasing attention due to their promising applications in various fields such as catalysis, adsorption, separation, and controlled bimolecular/drug release.<sup>1</sup> HPS with multiple pore sizes provide advantages over monomodal porous structures, which may provide diverse pathways to control mass transport and allow for high loading of target molecules.

The synthesis of HPS with macroporous cavities and mesopores shells has been well-documented, which can be obtained generally through colloidal templating,<sup>2</sup> emulsion templating,<sup>3</sup> or multisurfactant templating.<sup>4</sup> Djopoputro et al.<sup>5</sup> reported the synthesis of organosiliceous vesicles with ordered mesoporous organosilica wall using fluorocarbon/hydrocarbon surfactants as the structural directing agents through a vesicle templating (VT)<sup>6</sup> and liquid-crystal templating (LCT)<sup>7</sup> dual-templating approach. Yang et al.<sup>8</sup> reported a facile synthesis of siliceous nanopods with inner multilamellar core and outer hexagonal wall architectures by adjusting the mass ratio of perfluorooctanoic acid (PFOA)/cetyltrimethylammonium bromide (CTAB) from a compromised VT-LCT dual-templating method. More recently, through the surface sol-gel process on the polystyrene-*co*-poly(4-vinylpyridine) (PS-*co*-P4VP) and CTAB core-shell templates, the hollow mesoporous silica microspheres with controllable wall thickness can be obtained.<sup>9</sup> However, the pore sizes in the outer shell are generally small (<5 nm) in previous reports. So far there have been few reports concerning the synthesis of HPSs with large pore shells. Yeh and co-workers reported the synthesis of hollow silica spheres with disordered mesostructured shells and pore size of about 5.5–7.5 nm.<sup>4a</sup> It is a challenge to synthesize HPSs with large pore shells and ordered mesostructures.

Herein, we report a simple one-step synthesis of HPS with multilamellar vesicular core and ordered mesostructured shell using a nonionic block copolymer [Pluronic P123, EO<sub>20</sub>PO<sub>70</sub>-EO<sub>20</sub>, where EO is poly(ethylene oxide) and PO is poly(propylene oxide)] and sodium perfluorooctanoate (PFONa) as cotemplates through a dual-templating approach. The multilamellar vesicular core has cavity size generally larger than 100 nm and a layer-layer distance of ca. 10 nm. Moreover, the shell of HPS has an ordered hexagonal mesostructure, and the pore size of the shell is as large as 9.8 nm.

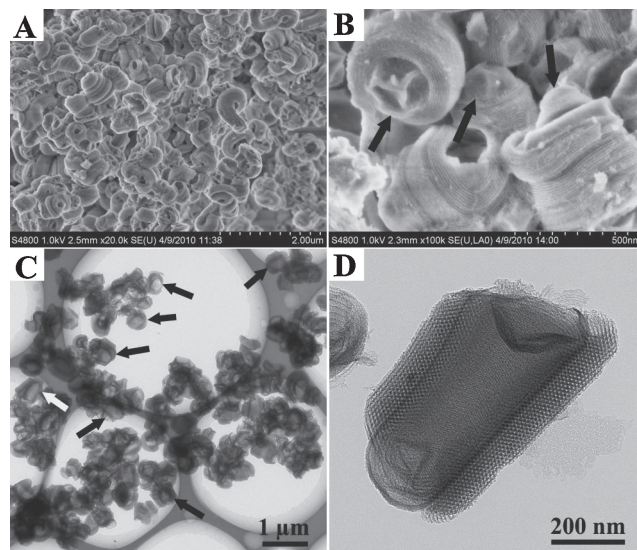


**Figure 1.** The low- and high-magnification SEM (A, B) and TEM (C, D) images of HPSs. The arrows in (B) indicate the irregular-shaped cores and the arrows in (C) show the large hollow cores.

HPSs were synthesized in a strong acid solution at 50 °C with a PFONa/P123 molar ratio (*R*) of 1.33 (see Supporting Information). Scanning electron microscopy (SEM) at a low-magnification shows a high yield of donutlike particles (Figure 1A). At a higher magnification, it is shown that the donutlike morphology consists of concentric pore channels (Figure 1B). Interestingly, the middle of the donutlike morphology is not empty, and the ordered pore channels grow around an irregular-shaped core (indicated by arrows) to form a complex core-shell structure. Transmission electron microscopy (TEM) was employed to observe the detailed core-shell structure. Figure 1C is a large area TEM image displaying the nature of hollow particles. The high-magnification TEM image exhibits an elongated vesicle as the core surrounded by highly ordered hexagonally packed mesoporous silica as the shell (Figure 1D). To further confirm the hexagonal mesostructure of the shell, a series of tilted TEM images for one typical HPS particle were acquired (Figure S1<sup>13</sup>). When the tilted axis is perpendicular to the long axis of the particle, the hexagonal pattern on both sides of the shell can be clearly seen at a tilt angle of 0°, while the stripelike pattern can be observed at high tilt angles such as ±40°. These results indicate that the hexagonally patterned pore channels are wrapped around the long axis of the HPS particle.

Although the shell structure can be determined by conventional TEM, detailed information of the core cannot be clearly

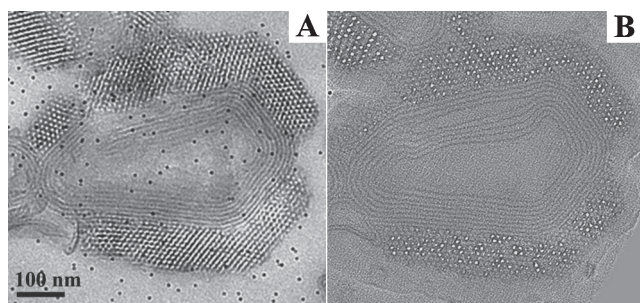


**Figure 2.** The representative cross-section TEM image of a typical HPS particle (A) and an ET slice (B). The black dots are gold fiducial markers for ET alignment.

demonstrated due to the thickness of the shell (ca. 100 nm) and overlapping effect. Therefore, an ultramicrotome was employed to prepare thin sections (ca. 100 nm) for TEM observations. Figure 2A is a representative cross-section TEM image of an HPS particle showing a multilamellar vesicular core and an ordered hexagonal array shell viewed along the pore direction. To observe the inner core structure more clearly, electron tomography (ET)<sup>10</sup> was performed and an ET slice is displayed in Figure 2B, revealing that the core is a closed multilamellar vesicle with an average layer–layer distance of ca. 10 nm. Comparison between Figures 1D and 2 show the advantage of ET in revealing the core structure of complex core–shell morphologies.

The X-ray diffraction (XRD) pattern of the calcined HPS exhibits three well-resolved Bragg peaks indexed as the 10, 11, and 20 reflections of a *p6mm* plane group (Figure 3A). The N<sub>2</sub> sorption isotherm presents a capillary condensation at  $P/P_0 = 0.75$ – $0.85$ , corresponding to a relatively narrow pore size distribution of 9.8 nm (inset of Figure 3B). The surface area and pore volume are  $444 \text{ m}^2 \text{ g}^{-1}$  and  $0.79 \text{ cm}^3 \text{ g}^{-1}$ , respectively.

To understand the formation mechanism of HPS, samples synthesized at different PFONa/P123 *R* are investigated. SEM and TEM images demonstrate a morphological and structural transition from rodlike morphology with ordered hexagonal structure ( $R = 0$ ) to hexagonal mesoporous curved rods mixed with few multilamellar vesicular structures ( $R = 0.67$ ) and then to the aggregated multilayered vesicles ( $R = 2.00$ , Figure S2<sup>13</sup>). The structures of these samples are further determined by the XRD patterns and N<sub>2</sub> sorption isotherms (Figure S3<sup>13</sup>), and their physicochemical parameters are summarized in Table S1.<sup>13</sup>

The structural transition is similar to a previous study,<sup>11</sup> in which prefluorocarbon molecules are embedded in the PEO moiety to adjust the hydrophilic/hydrophobic volume ratio ( $V_H/V_L$ ) and eventually the templated mesostructure. Compared to our previous work,<sup>11</sup> the initial synthetic temperature was raised from 35 to 50 °C in this study, thus the PEO chains are more dehydrated and more hydrophobic, leading to slightly enlarged pore sizes<sup>11</sup> and increased packing parameter of self-assembled mesostructure.<sup>12</sup> As a result, the hexagonal to vesicle structural transition occurs at a lower PFONa/P123 *R* of 0.67 (compared to 1.4 in our previous study<sup>11</sup>), and HPS with a core/shell structure occurred at  $R = 1.33$ . It is proposed that the multilamellar vesicle is formed through a VT process, and the ordered hexagonal mesostructure assembled through a LCT mechanism grows around the multilamellar core, giving rise to HPS with core–shell structure by a dual-templating approach.<sup>5,8</sup>

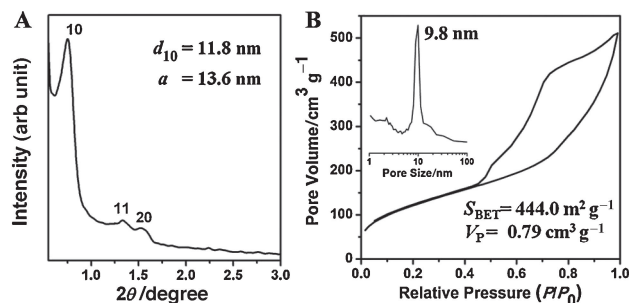


**Figure 3.** XRD pattern (A), N<sub>2</sub> sorption isotherm (B), and pore size distribution (inset) of the calcined HPSs.

In conclusion, HPSs with multilamellar vesicular core and ordered mesostructured shell have been successfully synthesized using a simple one-step method. The large cavity ( $> 100 \text{ nm}$ ) and large pore size in the shell (ca. 10 nm) of this material are expected to find applications in loading and controlled release of large molecules.

We thank the Australian Research Council and the Australian Government's ISL program.

#### References and Notes

- a) Q. Huo, J. Liu, L.-Q. Wang, Y. Jiang, T. N. Lambert, E. Fang, *J. Am. Chem. Soc.* **2006**, *128*, 6447. b) Y. T. Lim, J. K. Kim, Y.-W. Noh, M. Y. Cho, B. H. Chung, *Small* **2009**, *5*, 324. c) Y.-S. Lin, C. L. Haynes, *Chem. Mater.* **2009**, *21*, 3979. d) E. Climent, A. Bernardos, R. Martínez-Mañez, A. Maquieira, M. D. Marcos, N. Pastor-Navarro, R. Puchades, F. Sancenón, J. Soto, P. Amorós, *J. Am. Chem. Soc.* **2009**, *131*, 14075.
- a) F. Caruso, R. A. Caruso, H. Möhwald, *Science* **1998**, *282*, 1111. b) N. Kato, T. Ishii, S. Koumoto, *Langmuir* **2010**, *26*, 14334.
- a) N. E. Botterhuis, Q. Sun, P. C. M. M. Magusin, R. A. van Santen, N. Sommerdijk, *Chem.—Eur. J.* **2006**, *12*, 1448. b) J. Li, J. Liu, D. Wang, R. Guo, X. Li, W. Qi, *Langmuir* **2010**, *26*, 12267. c) J. Wang, Q. Xiao, H. Zhou, P. Sun, Z. Yuan, B. Li, D. Ding, A.-C. Shi, T. Chen, *Adv. Mater.* **2006**, *18*, 3284.
- a) Y.-Q. Yeh, B.-C. Chen, H.-P. Lin, C.-Y. Tang, *Langmuir* **2006**, *22*, 6. b) J. Liu, S. B. Hartono, Y. G. Jin, Z. Li, G. Q. Lu, S. Z. Qiao, *J. Mater. Chem.* **2010**, *20*, 4595.
- H. Djojoputro, X. F. Zhou, S. Z. Qiao, L. Z. Wang, C. Z. Yu, G. Q. Lu, *J. Am. Chem. Soc.* **2006**, *128*, 6320.
- D. H. W. Hubert, M. Jung, P. M. Frederik, P. H. H. Bomans, J. Meuldijk, A. L. German, *Adv. Mater.* **2000**, *12*, 1286.
- C. T. Kresge, M. E. Leonowicz, W. J. Roth, J. C. Vartuli, J. S. Beck, *Nature* **1992**, *359*, 710.
- S. Yang, X. Zhou, P. Yuan, M. Yu, S. Xie, J. Zou, G. Q. Lu, C. Yu, *Angew. Chem., Int. Ed.* **2007**, *46*, 8579.
- S. Wang, M. Zhang, D. Wang, W. Zhang, S. Liu, *Microporous Mesoporous Mater.* **2011**, *139*, 1.
- P. Yuan, N. Liu, L. Zhao, X. Zhou, L. Zhou, G. J. Auchterlonie, X. Yao, J. Drennan, G. Q. Lu, J. Zou, C. Yu, *Angew. Chem., Int. Ed.* **2008**, *47*, 6670.
- P. Yuan, S. Yang, H. Wang, M. Yu, X. Zhou, G. Lu, J. Zou, C. Yu, *Langmuir* **2008**, *24*, 5038.
- a) M. S. Bakshi, P. Bhandari, *J. Photochem. Photobiol., A* **2007**, *186*, 166. b) T. Klimova, A. Esquivel, J. Reyes, M. Rubio, X. Bokhimi, J. Aracil, *Microporous Mesoporous Mater.* **2006**, *93*, 331.
- Supporting Information is available electronically on the CSJ-Journal Web site, <http://www.csj.jp/journals/chem-lett/index.html>.